Neuropsychopharmacology (2018) 43, 393–405

www.neuropsychopharmacology.org

Failure to Inactivate Nuclear GSK3β by Ser^{389}-Phosphorylation Leads to Focal Neuronal Death and Prolonged Fear Response

Tina M Thornton[1,7], Brendan Hare[2,7], Sandra Colié[3], William W Pendlebury[4], Angel R Nebreda[3,5], William Falls[2,8], Diane M Jaworski[6,8] and Mercedes Rincon[*,1,8]

[1]Department of Medicine/Immunobiology, University of Vermont, Burlington, VT, USA; [2]Department of Psychology, University of Vermont, Burlington, VT, USA; [3]Institute for Research in Biomedicine (IRB Barcelona), Barcelona Institute of Science and Technology, Barcelona, Spain; [4]Department of Pathology, University of Vermont, Burlington, VT, USA; [5]ICREA, Pg. Lluís Companys 23, Barcelona, Spain; [6]Department of Neurological Sciences, University of Vermont, Burlington, VT, USA

GSK3β plays an essential role in promoting cell death and is emerging as a potential target for neurological diseases. Understanding the mechanisms that control neuronal GSK3β is critical. A ubiquitous mechanism to repress GSK3β involves Akt-mediated phosphorylation of Ser^{9}. Here we show that phosphorylation of GSK3β on Ser^{389} mediated by p38 MAPK specifically inactivates nuclear GSK3β in the cortex and hippocampus. Using GSK3β Ser^{389} to Ala mutant mice, we show that failure to inactivate nuclear GSK3β by Ser^{389} phosphorylation causes neuronal cell death in subregions of the hippocampus and cortex. Although this focal neuronal death does not impact anxiety/depression-like behavior or hippocampal-dependent spatial learning, it leads to an amplified and prolonged fear response. This phenotype is consistent with some aspects of post-traumatic stress disorder (PTSD). Our studies indicate that inactivation of nuclear GSK3β by Ser^{389} phosphorylation plays a key role in fear response, revealing new potential therapeutic approaches to target PTSD.
Neuropsychopharmacology (2018) **43,** 393–405; doi:10.1038/npp.2017.187; published online 20 September 2017

INTRODUCTION

Glycogen synthase kinase (GSK)-3 is a highly expressed serine–threonine protein kinase present in all cells but is particularly abundant in the central nervous system (CNS) (Woodgett, 1990). GSK3β is mainly a cytoplasmic protein. However, it has been shown to accumulate within the nucleus in response to certain stimuli, although the function of nuclear GSK3β is not well understood (Bijur *et al*, 2000; Bijur and Jope, 2003). There are two GSK3 isoforms, GSK3α and GSK3β, encoded by separate genes. Although they share significant homology within the kinase domain, their function and/or expression is not fully redundant based on the finding that deletion of GSK3β, but not GSK3α, results in embryonic lethality (Hoeflich *et al*, 2000). GSK3 was first identified as a kinase that phosphorylates and negatively regulates glycogen synthase (Embi *et al*, 1980; Frame and Cohen, 2001), but in the many systems where it has been studied, one major consequence of active GSK3β is cell death (Jacobs *et al*, 2012). In the CNS, loss of GSK3 results in brain abnormalities, neuronal hyperproliferation, and excess survival (Kim *et al*, 2009). In addition, hyper-activation of GSK3β in neuronal cells increases cell death in response to cell stress (Bijur *et al*, 2000). Increased neuronal cell death caused by enhanced GSK3 activity has been thought to contribute to human neurological disorders, such as Huntington disease, Alzheimer's disease, and bipolar disorder (Carmichael *et al*, 2002; Cai *et al*, 2012; Cole, 2013). Increased GSK3β activity has been shown to mediate tau hyperphosphorylation, β-amyloid-induced neurotoxicity, and mutant presenilin-1 pathogenic effects in Alzheimer's disease (Jope and Johnson, 2004). Inhibitors of GSK3 have shown promise in mouse models of Alzheimer's disease (Noble *et al*, 2005; Rockenstein *et al*, 2007; Eldar-Finkelman and Martinez, 2011) and some have been tested in clinical trials for Alzheimer's disease (Lovestone *et al*, 2015). Lithium, commonly used in the treatment of bipolar disorder, stabilizes mood in part through the inhibition of GSK3 activity (Jope, 2011). GSK3β inactivation has also been implicated mechanistically in the antidepressant effect of ketamine (Beurel *et al*, 2011; Liu *et al*, 2013; Chiu *et al*, 2015). Thus, determining the mechanisms that regulate GSK3 activity in CNS is highly relevant.

Unlike most kinases, GSK3 is constitutively active. A widely studied mechanism for GSK3 inhibition is through phosphorylation of Ser^{9} on GSK3β and Ser^{21} on GSK3α primarily by Akt (Cross *et al*, 1995). The phosphorylated N-terminus of GSK3β at Ser^{9} acts as a competitive inhibitor by folding into the active site and preventing substrate binding (Frame *et al*, 2001). Phosphorylation of Ser^{9}/Ser^{21}

*Correspondence: Dr M Rincon, Department of Medicine/Immunobiology Program, University of Vermont, Given Medical Building D305, 89 Beaumont Ave., Burlington, VT 05405, USA, Tel: 802 656-0937, Fax: 802 656-3854, E-mail: mrincon@uvm.edu
[7]Co-first authors.
[8]These authors contributed equally to this work.
Received 11 May 2017; revised 25 July 2017; accepted 17 August 2017; accepted article preview online 23 August 2017

can be detected constitutively in most cells, but it can be further increased by insulin, growth factors, and cellular stress signaling (Doble and Woodgett, 2003). Studies with double knockin (KI) mice in which Ser^{9} in GSK3β and Ser^{21} in GSK3α were mutated to Ala have shown the relevance of this mechanism for inactivation of muscle glycogen synthase by insulin (McManus *et al*, 2005), but not for the inactivation of GSK3 through WNT/β-catenin signaling (McManus *et al*, 2005). WNT signaling promotes sequestration of GSK3 in multivesicular endosomes and the generation of lipoprotein receptor-related protein pseudo-substrates (Niehrs and Acebron, 2010). Interestingly, the loss of inhibitory serine phosphorylation in GSK3 Ser^{9}Ala/Ser^{21}Ala double KI mice did not affect neuronal survival *in vitro* or *in vivo* (Hongisto *et al*, 2008; Eom and Jope, 2009) further supporting the existence of an alternative neuronal protection mechanism to regulate GSK3β in the brain.

Recently, we identified another direct inhibitory phosphorylation pathway for GSK3β, but not for GSK3α (Thornton *et al*, 2008). p38 MAPK inactivates GSK3β by phosphorylation of Thr^{390} in human GSK3β or Ser^{389} in mouse GSK3β (Thornton *et al*, 2008). This phosphorylation by p38 MAPK results in a similar degree of GSK3β activity inhibition as Ser^{9} phosphorylation by Akt (Thornton *et al*, 2008). Thr^{390}/Ser^{389} is located at the very end of the GSK3β C-terminus, which is also very flexible in structure, similar to the N-terminus where Ser^{9} is located (Dajani *et al*, 2001). Thus, the mechanism of inactivation upon phosphorylation at the C-terminus is also likely through folding into the active site and competing for substrate binding. However, these two mechanisms for GSK3β inactivation are independent, respond to different stimuli, and target different pools of GSK3β (Thornton *et al*, 2016). While phosphorylation of Ser^{9} is ubiquitously present in most tissues, Ser^{389} phosphorylation is more restricted to specific tissues (eg, brain, thymus, and spleen) under physiological conditions (Thornton *et al*, 2008). In addition, Ser^{9} phosphorylation of GSK3β occurs primarily in the cytosol, but we have recently shown that Ser^{389} phosphorylation targets nuclear GSK3β (Thornton *et al*, 2016). Importantly, phosphorylation of GSK3β at Ser^{389} is specifically triggered in response to DNA double-strand breaks (DSB) induced by external stimuli as well as by naturally generated DSB arising from V(D)J recombination and class switch recombination in T and B lymphocytes (Thornton *et al*, 2016). The major function of Ser^{389} GSK3β phosphorylation in these cells is to prevent cell death, primarily through necroptosis caused by DSB (Thornton *et al*, 2016).

Although phosphorylation of GSK3β at Ser^{389} is selectively abundant in the brain under physiological conditions (Thornton *et al*, 2008), the function of this mechanism of GSK3β regulation in the brain is unknown. Here we show that phosphorylation of GSK3β at Ser^{389} is a mechanism to inactivate the nuclear pool of GSK3β within the brain. Failure to inactivate nuclear GSK3β in Ser^{389}Ala mutant mice causes the death of a subset of neurons in the cortex and hippocampus. While spatial memory and anxiety/depression-like behaviors are not impaired, Ser^{389}Ala GSK3β KI mice display augmented fear-conditioning behavior, a phenotype commonly observed in stress-associated diseases such as post-traumatic stress disorder (PTSD). Thus, inactivation of GSK3β through Ser^{389} phosphorylation could be a novel approach for the treatment of PTSD-like symptoms.

MATERIALS AND METHODS

Mice

C57BL/6 GSK3β KI mice have been previously described (Thornton *et al*, 2016). Wild-type mice (WT) were purchased from Jackson Laboratories (Bar Harbor, ME). Mice deficient for p38α MAPK specifically in neurons (p38αΔ-N) were generated as described (Colié *et al*, 2017). p38α floxed homozygous mice were crossed with p38α floxed homozygous CAMKII-CRE positive mice to generate p38α floxed homozygous mice plus (p38αΔ-N) or minus (WT) a single copy of the CAMKII-CRE transgene. All procedures were approved by the University of Vermont Animal Care and Use Committee.

Behavioral Tasks

A cohort of male and female WT and GSK3β KI mice ($n=5$ females, 5 males per genotype) were examined in the behavioral tasks described below. The order of testing was acoustic startle, open field, zero maze, auditory fear conditioning, terminating with forced swim. A separate cohort was used for the water maze experiment ($n=8$ females, 7 males per genotype). The following behavioral tasks were performed: (1) open field and zero maze, (2) water maze, (3) forced swim, and (4) auditory fear conditioning. Experimental detail is provided in the 'Extended Methods' in the Supplementary Information section.

Western Blot Analysis

Whole-cell extracts were prepared in Triton lysis buffer and used for western blot analysis as we previously described (Derijard *et al*, 1994; Rincon *et al*, 1997). Nuclear and cytosolic extracts were prepared as previously described (Schreiber *et al*, 1989; Tugores *et al*, 1992). For co-immunoprecipitation, nuclear extracts were prepared as previously described (Jamil *et al*, 2010). ExactaCruz F Immunoprecipitation Kit (Santa Cruz Biotechnology) was used for immunoprecipitation/western blot analysis with rabbit antibodies. Anti-actin, anti-GAPDH, and anti-GSK3β were purchased from Santa Cruz Biotechnology. Anti-phospho-Ser^{9} GSK3β, anti-phospho-Mcl1, and anti p38α MAPK were purchased from Cell Signaling Technology (Danvers, MA). Anti-phospho-S^{389} GSK3β and anti-TUJ1 was purchased from Millipore (Billerica, MA). Anti-phospho-Thr^{390} GSK3β rabbit polyclonal antibody has been described (Thornton *et al*, 2016). Anti-rabbit HRP and anti-mouse HRP (Jackson ImmunoResearch Laboratories) and anti-goat-HRP (Santa Cruz Biotechnology) were used as secondary antibodies. NIH ImageJ was used to quantify band intensity.

GSK3β Kinase Activity Assays

To determine whether S^{389} phosphorylation regulated a distinct component of GSK3β activity, kinase assays were

conducted. GSK3β was immunopreciptitated from cerebral cortex protein lysates and kinase activity was determined as previously published (Thornton *et al*, 2008).

Immunolabeling

The primary antibodies used included rabbit anti-phospho-Ser^{389} or anti-phospho-Thr^{390} GSK3β polyclonal antibodies, Anti-NeuN (Millipore), anti-TUJ1, anti-rabbit Alexa Fluor 568 (Invitrogen) or Cy3 (Jackson ImmunoResearch). DAPI was used as a nuclear stain. Images of cells were acquired on a Zeiss LSM-510. Staining of human tissue was performed as previously described (Long *et al*, 2011). Images were acquired with identical exposure settings using a SPOT RT digital camera. Fluoro-Jade C (Millipore) staining was performed according to the manufacturer's instructions.

Statistical Analysis

Data are expressed as means ± standard error of the mean. Behavioral analysis utilized mixed model ANOVAs followed by LSD protected *t*-tests. Initial analysis included sex. However, we observed no sex differences; therefore, sex was left out of the analysis that follows. Results were analyzed by SPSS software version 22 (IBM; Armonk, NY). $P<0.05$ was considered statistically significant.

RESULTS

Ser^{389} Phosphorylation of GSK3β Selectively Targets the Nuclear Pool of GSK3β in the Brain

The regulation of GSK3β by Ser^{9} phosphorylation occurs in all tissues as a default pathway to restrain GSK3β activity (Jope and Johnson, 2004). In contrast, phospho-Ser^{389} GSK3β is highly abundant in the brain (Thornton *et al*, 2008). To determine the distribution of phospho-Ser^{389} GSK3β within the brain, western blot analysis was performed using lysates from different regions of the brain. While phospho-Ser^{9} GSK3β was abundant in all regions of the brain examined, higher levels of phospho-Ser^{389} GSK3β were detected in the cortex and hippocampus (Figure 1a). To address whether phosphorylation of Ser^{389} and phosphorylation of Ser^{9} represented alternative pathways to control two independent spatial pools of GSK3β we performed immunoprecipitation analysis. Whole-cell extracts from the cerebral cortex were used to immunoprecipitate phospho-Ser^{9} GSK3β, and both the immunoprecipitate and flow-through were examined by western blot analysis. As expected, phospho-Ser^{9} was abundantly present in the immunoprecipitates, but not in the flow-through (Figure 1b). In contrast, phospho-Ser^{389} was not detected in the phospho-Ser^{9} immunoprecipitates, but was abundantly present in the flow-through (Figure 1b), indicating that the phospho-Ser^{9} GSK3β pool is not phosphorylated at Ser^{389}. Analysis of total GSK3β revealed that only a fraction of GSK3β was actually phosphorylated on Ser^{9} since large amounts of GSK3β were still present in the flow-through after phospho-Ser^{9} immunoprecipitation (Figure 1b). Thus, phosphorylation of GSK3β on Ser^{389} targets an independent pool of GSK3β in the brain that is not phosphorylated on Ser^{9}.

We have recently shown that Ser^{389} phosphorylation primarily regulates nuclear GSK3β in lymphocytes (Thornton *et al*, 2016). We, therefore, examined the subcellular distribution of phospho-Ser^{389} GSK3β in mouse cerebral cortex by immunostaining and confocal microscopy. The immunostaining revealed a punctate nuclear

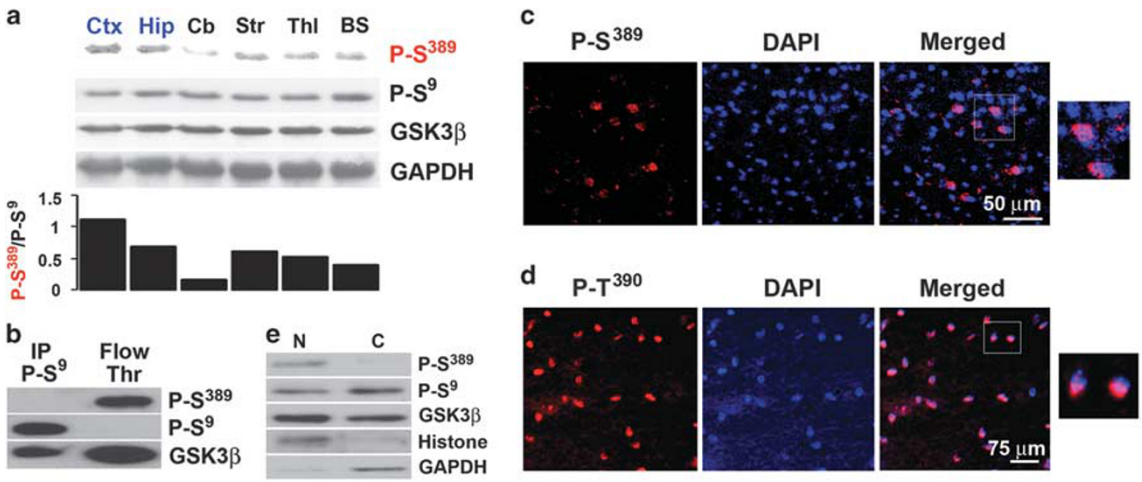

Figure 1 Ser^{389}/Thr^{390} phosphorylation of nuclear GSK3β in regions of the brain. (a) Whole-cell lysates from different regions of wild-type (WT) mouse brain (BS, brain stem; Cb, cerebellum; Ctx, cerebral cortex; Hip, hippocampal formation; Str, striatum; Thl, thalamus) were examined for P-Ser^{389}GSK3β, P-Ser^{9} GSK3β and total GSK3β by western blot analysis. GAPDH is shown as a loading control. The ratio of P-Ser^{389} to P-Ser^{9} are shown for comparison. (b) P-Ser^{9} GSK3β was immunoprecipitated from mouse cerebral cortex extracts. P-Ser^{389}GSK3β, P-Ser^{9} GSK3β, and total GSK3β in the immunoprecipitate (P-S^{9} IP) or the flow-through (Flow Thr) left were examined by western blot analysis. (c) The presence of P-Ser^{389} (red) and DAPI nuclear staining (blue) in mouse cerebral cortex were examined by immunostaining and microscopy. Cells in white boxes are shown enlarged to show cellular localization. (d) The presence of P-Thr^{390} (red) and DAPI nuclear staining (blue) in the post-mortem human cerebral cortex were examined by immunostaining and microscopy. Cells in white boxes are shown enlarged to show cellular localization. (e) Western blot analysis using nuclear (N) and cytosolic (C) extracts from the mouse cortex were analyzed by western blot for P-Ser^{389} GSK3β, P-Ser^{9} GSK3β and total GSK3β. GAPDH and Histone are shown as controls for the cytoplasmic and nuclear fractions, respectively.

distribution of phospho-Ser^{389} GSK3β in a subset of cells (Figure 1c). Similarly, immunofluorescence staining of post-mortem human brain tissue for phospho-Thr^{390} GSK3β (human equivalent of mouse Ser^{389}) revealed a primarily nuclear staining (Figure 1d). In addition, western blot analysis using nuclear and cytosolic extracts from the cerebral cortex further confirmed the presence of phospho-Ser^{389} GSK3β in the nuclear fraction, whereas it was practically undetectable in the cytosol (Figure 1e). Thus, unlike phosphorylation of Ser^{9}, phosphorylation of Ser^{389} targets specifically the nuclear pool of GSK3β in the brain.

Phosphorylation of GSK3β on Ser^{389} is Required to Restrain the Activity of Nuclear GSK3β in the Brain

To investigate the role of GSK3β Ser^{389} phosphorylation in the brain, we used GSK3β Ser^{389}Ala knockin (GSK3β KI) mice where Ser^{389} was replaced with Ala to prevent the phosphorylation of this residue and block the regulation of GSKβ by this mechanism (Thornton *et al*, 2016). Western blot analysis confirmed the absence of phospho-Ser^{389} GSK3β in the whole brain from homozygous GSK3β KI mice while normal levels were present in heterozygous GSK3β KI mice (Figure 2a). Ser^{9} phosphorylation of GSK3β was not affected by the Ser^{389}Ala mutation (Figure 2a), further demonstrating that these two pathways are independent of each other. No discernible differences in gross brain anatomy were observed between GSK3β KI mice and WT mice (Figure 2b). Immunostaining analysis with NeuN and class III β-tubulin/Tuj1, two standard markers for neurons, did not show drastic differences in the density of neurons within the cerebral cortex and hippocampus of WT and GSK3β KI mice (Figure 2c). Thus, blocking Ser^{389} phosphorylation does not have a major effect on neuronal homeostasis in the brain.

To show that phosphorylation on Ser^{389} contributes to restrain the kinase activity of GSK3β in the brain, we measured GSK3β kinase activity in brain tissue from WT and GSK3β KI mice. Despite the already high kinase activity, we could detect a significant increase in kinase activity in extracts from GSK3β KI mice compared with the activity in WT mice (Figure 2d). To address the role of Ser^{389} phosphorylation of GSK3β on the activity of the nuclear vs the cytosolic pool of GSK3β, we examined GSK3β activity in nuclear and cytosolic extracts from the brains of WT and GSK3β KI mice. Consistent with the nuclear localization of phospho-Ser^{389} GSK3β, nuclear GSK3β activity was significantly elevated in GSK3β KI mice compared with WT mice (Figure 2e). In contrast, cytosolic GSK3β activity was not increased in GSK3β KI mice (Figure 2e). Thus, phosphorylation of GSK3β on Ser^{389} is a mechanism to inactivate nuclear GSK3β in the brain.

Phosphorylation of GSK3β on Ser^{389} is Required for Survival of a Neuronal Subset in the Cortex and Hippocampus

Enhanced GSK3β activity has been shown to promote neuronal cell death (Bijur *et al*, 2000). Although the gross anatomy of the GSK3β KI brains was not altered (Figure 2b),

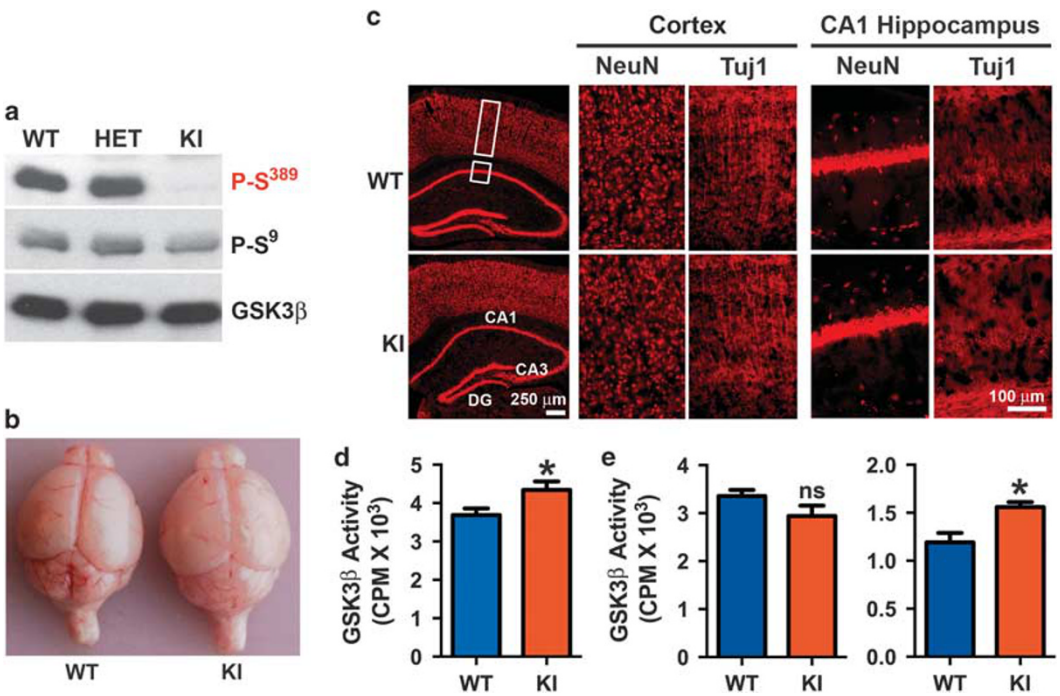

Figure 2 Increased nuclear GSK3β activity in the brain of GSK3β Ser^{389}Ala KI mice. (a) Whole-cell lysates from brains of WT, heterozygous (Het), and homozygous GSK3β KI mice were analyzed by western blot analysis for P-Ser^{389} GSK3β, P-Ser^{9} GSK3β, and total GSK3β. (b) Brains from WT and GSK3β KI mice. (c) Immunostaining for NeuN and Tuj1 (class II β-tubulin), as markers of mature neurons in WT and GSK3β KI cerebral cortex and hippocampal formation. The location of CA1, CA3, and the dentate gyrus (DG) is shown. The white boxes indicate the regions that correspond to the magnified images that follow. (d) GSK3β kinase activity using lysates from the cerebral cortex of WT and GSK3β KI mice ($n=9$). (e) GSK3β kinase activity in nuclear and cytosolic extracts from the hippocampus of WT and GSK3β KI mice ($n=3$). (*) indicates P-value <0.05 as determined by t-test.

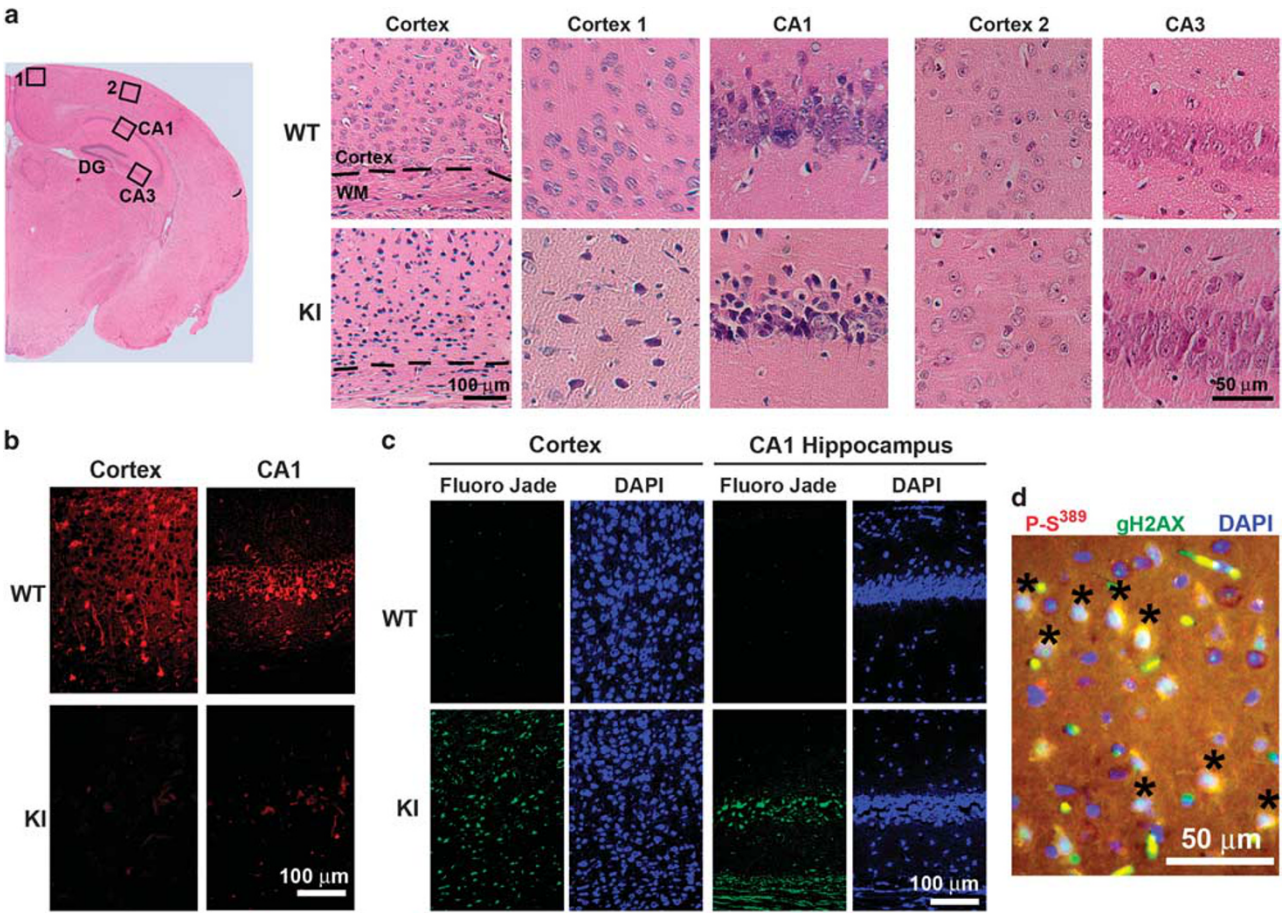

Figure 3 Impaired neuronal survival in GSK3β Ser^{389}Ala KI mice. (a) H&E-stained section of WT (low magnification). Box 1 indicates the region for 'Cortex 1' and box 2 indicates the region for 'Cortex 2'. The location of CA1, CA3, and the dentate gyrus (DG) are shown. Higher magnification of H&E-stained sections of WT and GSK3β KI cortex (1 and 2), and the hippocampal CA1 and CA3 sub-regions. (b) Immunostaining for phospho-Ser^{389} GSK3β in WT and GSK3β KI cerebral cortex and CAI hippocampal subregion. (c) Fluoro-Jade C (green) and DAPI (blue) staining of sections from WT and GSK3β KI cerebral cortex and hippocampal CA1 subregion. (d) Immunostaining of WT cortex for P-Ser^{389} (red), γH2AX (green), and DAPI nuclear staining (blue). Cells with co-staining for both P-Ser^{389} and γH2AX (white) are indicated by the asterisks (*).

histological examination of hematoxylin & eosin (H&E)-stained sections revealed the presence of some highly eosinophilic (darker) neurons with pyknotic nuclei in certain brain regions of GSK3β KI mice (Figure 3a). Eosinophilic neurons were particularly prominent in the cingulate and frontal cortices (Figure 3a—cortex 1 and Supplementary Figure S1), the CA1 region (Figure 3a), and dentate gyrus (Supplementary Figure S2) of the hippocampal formation, the amygdala and entorhinal cortex (Supplementary Figure S3) and the bed nucleus of the stria terminal and hypothalamus (data not shown). However, eosinophilic neurons were absent in other brain regions such as the parietal cortex (Figure 3a, cortex 2) and CA3 region of the hippocampus (Figure 3a) in GSK3β KI mice. The morphology of these cells is characteristic of what in human brain pathology is defined as 'dark neurons' and represents neurodegenerative cells (Garman, 2011). The restricted distribution of dark neurons suggests that neurons within a defined neuronal circuit are affected.

To examine whether the distribution of Ser^{389} phosphorylated GSK3β in WT mice correlated with the subregions where the dark neurons preferentially accumulate in GSK3β KI mice, we performed immunostaining for phospho-Ser^{389} GSK3β. The highest levels of phospho-Ser^{389} GSK3β immunostaining were found in the cerebral cortex and hippocampal regions of WT mice that correlated with the regions in GSK3β KI mice with a higher frequency of dark neurons (Figure 3b). The specificity of the phospho-Ser^{389} GSK3β staining was demonstrated by its absence in the brain of GSK3β KI mice (Figure 3b).

To demonstrate that the dark cells present in GSK3β KI brains represent degenerative neurons, brains sections from WT and GSK3β KI mice were stained with Fluoro-Jade C, the gold-standard dye used to visualize neurodegeneration (Schmued *et al*, 2005). Fluoro-Jade staining was practically undetectable in brains from WT mice as expected (Figure 3c). In contrast, clear Fluoro-Jade staining was present in regions of the cerebral cortex and hippocampus in GSK3β KI brain (Figure 3c), and these regions correlated with the areas where the dark cells were more abundant. We have previously shown that in response to endogenous DNA DSB phospho-Ser^{389} GSK3β co-localizes with γH2AX, a established marker for DSB (Thornton *et al*, 2016). A number of recent studies have revealed the presence of DSB

in neurons even during normal brain activity (Suberbielle *et al*, 2013; Madabhushi *et al*, 2015). To determine whether cells positive for phospho-Ser^{389} GSK3β contain DSB, we performed co-immunolabeling for phospho-Ser^{389} GSK3β and γH2AX. Phospho-Ser^{389} GSK3β and γH2AX co-localized in cells within the cingulate cortex indicating that cells positive for phospho-Ser^{389} GSK3β also contain DSB (Figure 3d and Supplementary Figure S4). Thus, inactivation of nuclear GSK3β through phosphorylation on Ser^{389} contributes to the fitness of a subset of neurons potentially undergoing DSB distributed in selective areas of the brain.

Conditional Deletion of p38a MAPK Results in Degeneration of a Neuronal Subset

Although Ser^{9} phosphorylation of GSK3β is mediated by Akt, Ser^{389} phosphorylation of GSK3β is mediated by p38 MAPK (Thornton *et al*, 2008, 2016). We investigated whether the failure to inactivate GSK3β through p38 MAPK could have a similar effect on neuronal survival. We used genetically modified mice with the p38α MAPK gene specifically disrupted in neurons (p38αΔ−N) through the expression of Cre recombinase under the control of the calcium/calmodulin-dependent protein kinase II (CAMKII) gene promoter (Colié *et al*, 2017). Western blot analysis confirmed the reduced expression of p38α MAPK in both the cortex and the hippocampus (Figure 4a). The gross brain morphology was not altered in p38αΔ−N mice (Figure 4b). Western blot analysis revealed a marked decrease of phospho-Ser^{389} GSK3β in lysates from p38αΔ−N mice compared with WT mice, indicating that phosphorylation of GSK3β at Ser^{389} in the brain is p38α MAPK dependent (Figure 4c). Examination of H&E staining revealed a higher frequency of dark neurons in the cortex of p38αΔ-N mice compared with WT mice (Figure 4d). In addition, increased numbers of Fluoro-Jade-positive cells were detected in the cortex of p38αΔ−N mice (Figure 4e and Supplementary Figure S5). Together these results show that loss of p38α MAPK correlates with decreased phosphorylation of GSK3β Ser^{389} and decreased survival of a subset of neurons similar to that found in GSK3β KI mice.

Failure to Inactivate GSK3β through Ser^{389} Phosphorylation in the Brain Promotes Death by Necroptosis

The best-characterized mechanism for GSK3β to mediate cell death is by phosphorylation of β-catenin in the cytosol, leading to the rapid degradation of this protein by APC complex (Filali *et al*, 2002; Liu *et al*, 2002). We examined whether the levels of β-catenin in the brain of GSK3β KI mice were decreased. Western blot analysis showed no difference in the levels of β-catenin between WT and GSK3β KI brains (Figure 5a). GSK3β can also promote cell death by the degradation of the pro-survival factor Mcl-1 through its phosphorylation on Ser^{159} (mouse Ser^{140}) (Maurer *et al*, 2006). Since Mcl-1 deficiency has also been shown to promote neuronal cell death in response to DSB (Arbour *et al*, 2008), we examined the levels of Mcl-1 in the brain in WT and GSK3β KI mice by western blot analysis. Interestingly, unlike β-catenin, Mcl-1 levels were strikingly decreased in GSK3β KI mice compared with WT mice (Figure 5a). To further show that increased GSK3β activity in these mice we examined phosphorylation of Mcl-1on Ser^{140}, the target for GSK3β. Despite the very low levels of Mcl-1 detected in GSK3β KI mice, the ratio of phosphorylated Mcl-1 was higher than in WT mice (Figure 5b). Thus, failure to inactivate nuclear GSK3β through this pathway results in

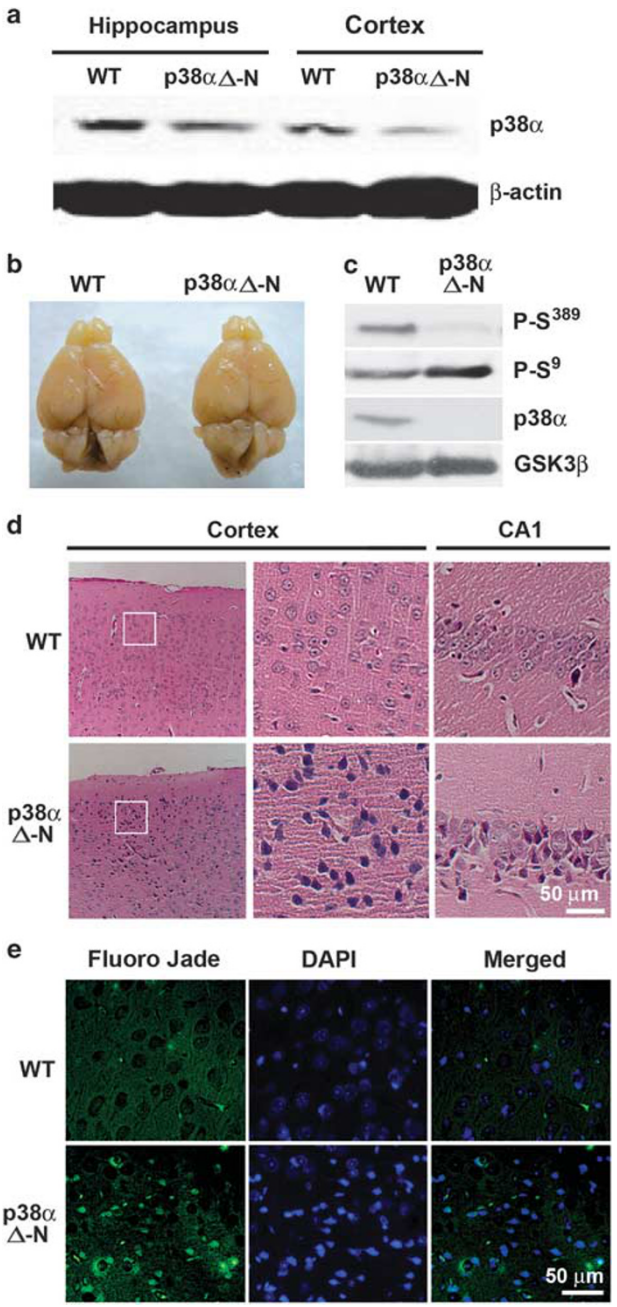

Figure 4 Neurodegeneration in neuronal-specific p38α MAPK KO mice. (a) Cell lysates from the cortex and hippocampus of WT and p38αΔ−N mice were analyzed by western blotting for p38α MAPK using actin as a loading control. (b) Representative pictures of brains from WT and p38αΔ-N mice. (c) Whole-cell lysates from brains of wild-type WT and p38αΔ-N mice were analyzed by western blot analysis for P-Ser^{389} GSK3β, p38α MAPK, P-Ser^{9} GSK3β, and total GSK3β. (d) H&E stained sections of WT and p38αΔ−N cerebral cortex and CA1. Boxed regions show the cortex area magnified (middle panels). (e) Fluoro-Jade C (green) and DAPI (blue) sections from WT and p38αΔ−N cerebral cortex.

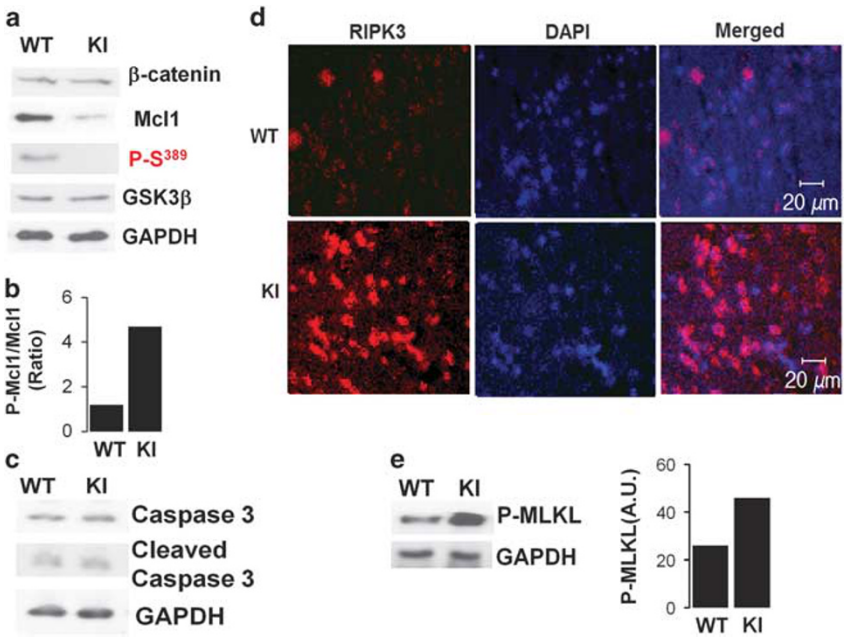

Figure 5 Decreased Mcl-1 and increased necroptosis in the brains of GSK3β S^{389}Ala KI mice. (a) β-catenin, Mcl-1, P-Ser^{389} GSK3β and total GSK3β were examined by western blot analysis in brain lysates from WT and GSK3β-KI mice. GAPDH is shown as a loading control. (b) Graph showing the ratio of P-Mcl-1 to Mcl-1 from the densitometry of western blots examining P-Mcl and Mcl in brain lysates from WT and GSK3β-KI mice. (c) Western blot analysis for caspase 3 in brain lysates from WT and GSK3β-KI mice. GAPDH is shown as a loading control. (d) The presence of RIPK3 (red) and DAPI nuclear staining (blue) in mouse cerebral cortex was examined by immunostaining and microscopy. (e) Western blot analysis for phospho-MLKL in brain lysates from WT and GSK3β-KI mice. GAPDH is shown as a loading control. The panel to the right displays the densitometry of phospho-MLKL.

increased phosphorylation and degradation of Mcl-1 in brain. Since mitochondrial Mcl-1 protects from apoptosis, we examine the presence of active caspase 3 by western blot analysis. However, the level of active caspase 3 was very low in brain, and there was no difference between WT and GSK3β KI mice (Figure 5c), suggesting that the neurodegeneration observed in GSK3β KI mice may not be through apoptosis.

In B cells from GSK3β KI mice, decreased levels of nuclear Mcl-1 have been associated with increased necroptosis (Thornton *et al*, 2016), an alternative pathway of death independent of mitochondria but dependent on the serine-threonine kinases RIPK1 and RIPK3 (Tait *et al*, 2014). Necroptosis has been found in some neurons where RIPK3 selectively translocates to the nucleus (Tait *et al*, 2014; Vitner *et al*, 2014). We, therefore, examined RIPK3 in brains from GSK3β KI mice by immunostaining and confocal microscopy analysis. Increased nuclear staining for RIPK3 was detected in the cerebral cortex of GSK3β KI mice compared with WT mice (Figure 5d and Supplementary Figure S6), supporting a greater magnitude of necroptosis in the GSK3β KI mice. In necroptosis, activated RIPK3 phosphorylates MLKL, one of the mediators of necroptosis that translocates to the membrane causing membrane rupture and death (Rodriguez *et al*, 2015). Analysis of phospho-MLKL by western blot analysis showed increased phospho-MLKL levels in GSK3β KI mice compared with WT mice (Figure 5e). Thus, taken together these data suggest that failure to inactivate GSK3β through Ser^{389} phosphorylation leads to increased necroptosis in some subregions of the brain.

Spatial Memory and Anxiety/Depression-like Behaviors are not Altered in GSK3β KI mice

The presence of pyknotic cells by H&E staining and fluoro-jade labeling in the hippocampus and cortex of GSK3β KI mice is consistent with localized neuronal degeneration. Given the hippocampal neurodegeneration detected, we assessed performance in the water maze, a hippocampal-dependent learning task (Morris *et al*, 1982). WT and GSK3β KI mice were trained to find a submerged platform over 8 days, with four trials per day. Performance improved over sessions (Day $f_{(2,56)} = 80.75$, $P < 0.0001$) though there was no effect of genotype (Genotype $f_{(1,28)} = 1.338$, $P > 0.05$) or interaction (Day × Genotype $f_{(2,56)} = 1.37$, $P > 0.05$), indicating that hippocampal spatial learning was similar in WT and GSK3β KI mice (Figure 6a). Spatial memory in the water maze can also be measured by utilizing a probe trial in which the platform is removed and the time spent in the general area of the platform is quantified. GSK3β KI and WT mice spent similar time searching in the platform quadrant ($t_{(28)} = 0.45$, $P > 0.05$) (Figure 6b). Additionally, the time spent searching in the appropriate quadrant was above chance in each group (WT $t_{(14)} = 3.61$, $P < 0.01$, KI $t_{(28)} = 3.36$, $P < 0.01$) (Figure 6b). Further, when the platform was moved to a new location, mice again performed similarly. Over four trials, distance travelled was reduced ($f_{(3,84)} = 9.97$, $P < 0.0001$), but there was no difference between the WT and GSK3β KI mice ($f_{(1,28)} = .44$, $P > 0.05$) or interaction ($f_{(3,84)} = 0.63$, $P > 0.05$) (Figure 6c).

Some reports indicate reduced hippocampal volume, indicative of neuronal atrophy, in the hippocampus of individuals with stress-associated diseases such as depression

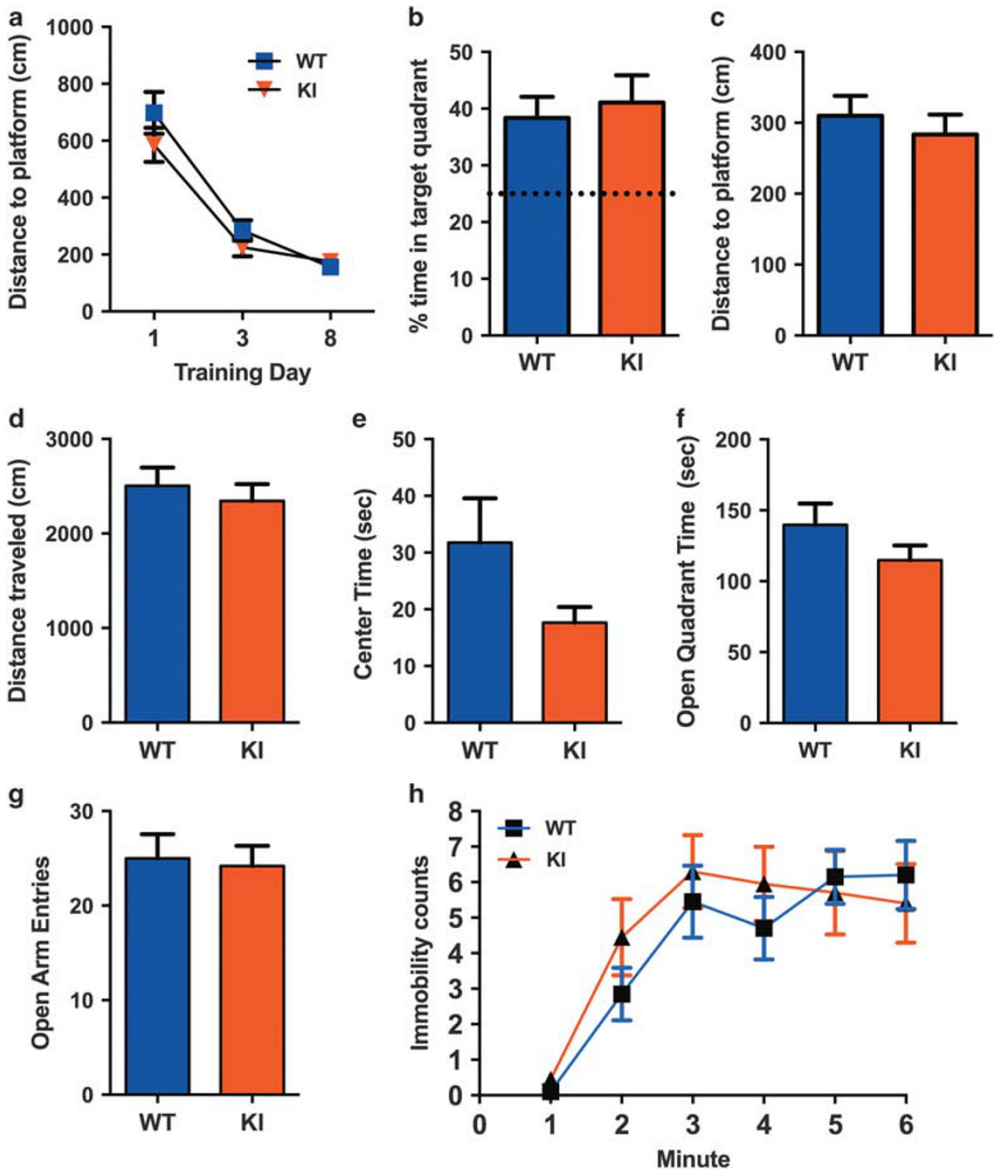

Figure 6 Hippocampal-dependent spatial memory and anxiety- and depression-like behaviors are not affected in GSK3β Ser389 KI mice. (a) The water maze is a spatial navigation task dependent on hippocampal integrity. Mice were trained to find a hidden platform over four trials each day for 8 days. (b) A probe trial, in which the platform is removed, can be used to assess memory for the platform location (dotted line represents chance performance). (c) The platform was moved to a new location for reversal trials to measure cognitive flexibility. (d) Locomotor activity and (e) center time during the open field test. (f) Time in the open quadrant and (g) and entries into the open quadrant during the zero-maze test. (h) Immobility time measured during a forced swim exposure. Data are mean ± SEM.

(Sheline *et al*, 1999). Therefore, the neuronal loss observed in the GSK3β KI mice could also affect anxiety and depression-like behavior. The open field test assesses both locomotor activity and anxiety-like behavior. When subjected to a 10-min open field test, GSK3β KI and WT mice traveled similar distances ($t_{(18)} = 0.61$, $P > 0.05$) (Figure 6d), indicating that locomotion was not affected in GSK3β KI mice. Further, each group entered the center of the arena equivalently ($t_{(18)} = 0.71$, $P > 0.05$), and spent equal time exploring the center of the open field ($t_{(18)} = 1.70$, $P > 0.05$) (Figure 6e), indicating similar anxiety levels between WT and GSK3β KI mice. The zero maze is another test for anxiety in which mice explore a raised circular track with enclosed portions in opposing quadrants over 5 min. Anxiety is defined as reduced open quadrant time or reduced open quadrant entries. Both open quadrant entries ($t_{(18)} = 0.63$, $P = 0.54$) (Figure 6f) and open quadrant time ($t_{(18)} = 0.85$, $P = 0.41$) (Figure 6g) were similar between GSK3β KI and WT mice providing further confirmation that anxiety-like behavior was similar between strains.

The forced swim test is a commonly used model of depression that measures behavioral despair through immobility, with increasing immobility time suggestive of increased depression (Bogdanova *et al*, 2013). An analysis of forced swim behavior by minute demonstrated that immobility increased in the later portions of the 6 min test (Minute $f_{(5,90)} = 24.54$, $P < 0.0001$), but there was no difference between GSK3β KI mice and WT mice ($f_{(1,18)} = 0.23$,

$P>0.05$) (Figure 6h). Thus, the regional neuronal degeneration observed in the GSK3β KI mice has no impact on locomotor activity, overall anxiety, or depression-like behavior.

Failure to Inactivate GSK3β through Ser^{389} Phosphorylation Causes an Exaggerated and Persistent Conditioning Fear

Reduced hippocampal volume has also been reported in individuals with PTSD (Gilbertson *et al*, 2002). Fear conditioning is highly conserved behavior that is defined by a fear response (eg, freezing in rodents) to a previously non-threatening stimulus (conditioned stimulus) that has been paired with an aversive stimulus (unconditioned stimulus). Dysregulated fear conditioning is a hallmark of stress exposure models used in rodents to model disorders such as PTSD (Izquierdo *et al*, 2006; Baran *et al*, 2009; Hoffman *et al*, 2014). Fear conditioning is dependent on the amygdala (LeDoux, 2003; Davis, 2006; Kim and Jung, 2006; Duvarci and Pare, 2014), but it is also influenced by the hippocampus through reciprocal connections between the two regions (Maren, 2001). We therefore investigated the response of GSK3β KI mice to auditory fear conditioning relative to WT mice. In this behavioral test, mice were given a series of pairings of a tone immediately followed by a mild foot shock in a distinctive context (ie, training chamber). Both GSK3β KI mice and WT mice displayed an increasing fear response to tone presentations subsequent to the first tone ($f_{(5,90)}=27.99$, $P<0.0001$) and there was no difference between the two groups ($f_{(1,18)}=1.06$, $P>0.05$) or interaction ($f_{(5,90)}=1.70$, $P>0.05$) (Figure 7a). Thus, acquisition of conditioned fear proceeded equivalently in GSK3β KI and WT mice. In order to test conditioned fear memory mice were given a pair of tests in a counterbalanced fashion beginning 24 h after conditioning and separated by 24 h. To test for an association between the training chamber and foot shock (contextual fear conditioning), mice were placed in the training chamber and allowed to explore without presentation of the tone. Interestingly, GSK3β KI mice clearly froze more than WT mice when placed into the training chamber ($t_{(18)}=3.18$, $P<0.01$) (Figure 7b). The association between the tone and the foot shock (auditory fear conditioning) was probed in a novel chamber where a 2-min baseline exploratory period was followed by the presentation of the tone that had previously been paired with foot shock. GSK3β KI mice also showed greater conditioned fear when the tone was presented in a novel context ($t_{(18)}=2.68$, $P<0.05$) (Figure 7c). Together these results suggest that the inability to phosphorylate Ser^{389} in GSK3β KI mice results in exaggerated fear conditioning to both contextual and auditory cues.

One component of PTSD is a pathological process by which overlapping features in a safe environment cause transfer of fear from a traumatic event (generalization) (American Psychiatric Association, 2000). Thus, to further examine the exaggerated fear behavior exhibited by GSK3β KI mice, we compared the first 2 min of behavior after mice were returned to the training chamber with the pre-tone baseline period in the novel chamber. During the first 2 min

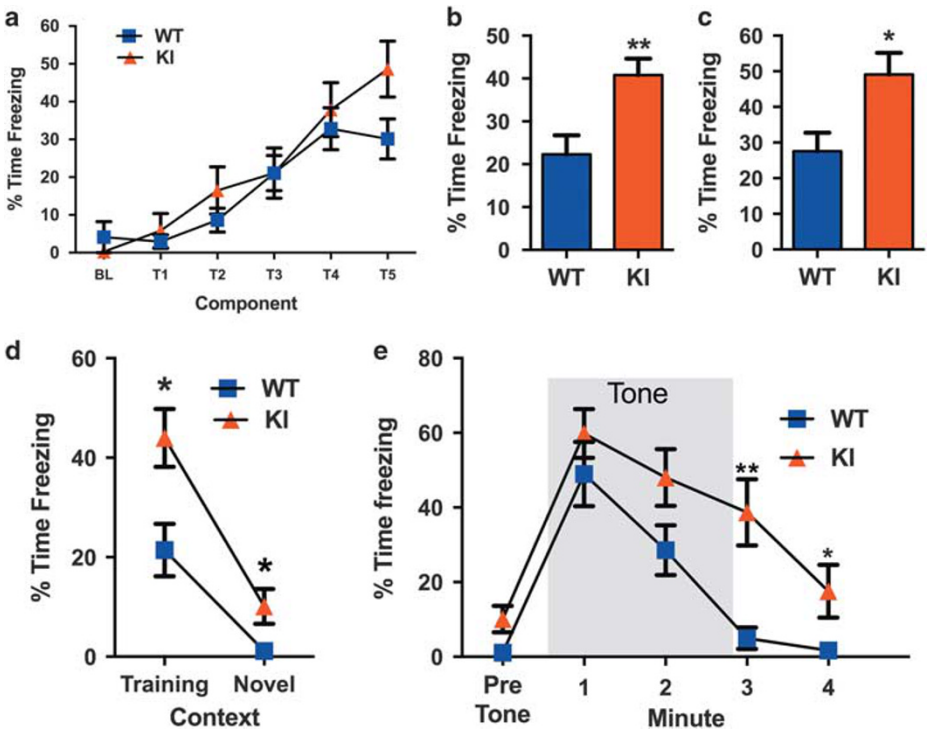

Figure 7 GSK3β S^{389}Ala KI mice show an exacerbated fear response. (a) Acquisition of fear conditioning during a training session with five tone-shock pairs. (b) Contextual fear expression upon return to the training context. (c) Tone fear expression during tone presentation in a novel context. (d) Fear expression immediately after exposure to the training context in comparison to expression upon placement into the novel context. (e) Time-dependent changes in tone fear expression during, and immediately after, the 3 min tone presentation in the novel context. Data are mean ± SEM, Significance was determined by *t*-test (*$P<0.05$, **$P<0.01$).

of re-exposure to the training context, GSK3β KI mice froze more than WT mice ($t_{(18)}=2.87$, $P<0.01$) (Figure 7d). Although discrimination between the novel chamber and training chamber was evident in both groups (GSK3β KI, $t_{(9)}=4.25$, $P<0.01$; WT, $t_{(14)}=3.86$, $P<0.01$) there was a clear transfer of fear in the GSK3β KI mice (Figure 7d). GSK3β KI mice spent more time freezing immediately after introduction to the novel context than WT mice ($t_{(9)}=2.53$, $P<0.05$) (Figure 7d). Thus, the enhanced fear conditioning observed in GSK3β KI mice is concurrent with an increased generalization of the fear conditioning experience.

Persistence of conditioned fear expression is also a feature of stress-associated disorders such as PTSD (Wessa and Flor, 2007). To examine the persistence of conditioned fear in GSK3β KI mice freezing was analyzed during each minute of the 3-min tone block in the novel chamber, as well as the final minute of the test following termination of the tone. The tone elicited substantial freezing above and beyond that elicited by the novel context alone (Figure 7e). GSK3β KI and WT mice froze similarly during the first 2 min of tone presentation. However, while the tone fear decayed rapidly in WT mice, fear was markedly persistent in GSK3β KI mice ($t_{(18)}=3.62$, $P<0.01$) (Figure 7e). This persistent fear was even evident during the minute after tone was terminated ($t_{(18)}=2.22$, $P<0.05$) (minute 4; Figure 7e). Together, these results show that the overall fear conditioning response is highly amplified and prolonged in GSK3β KI mice, a compelling phenotype given the focal hippocampal neurodegeneration observed GSK3β KI brains.

DISCUSSION

Although GSK3 was identified almost three decades ago, only during the last few years has it become one of the most prominent therapeutic targets, primarily in the areas of neurological diseases and cancer, as shown by the interest of the pharmaceutical industry and the number of published patents (Palomo and Martinez, 2016). Most approaches to regulating GSK3 activity are based on the best-characterized mechanism for GSK3 inactivation through Ser^{9} (GSK3β) or Ser^{21} (GSK3α) phosphorylation by Akt (Stambolic and Woodgett, 1994; Cross *et al*, 1995). However, we have previously shown that GSK3β, but not GSK3α, can also be inactivated by phosphorylation at the C-terminal Ser^{389} (mouse)/Thr^{390}(human) by p38 MAPK, and the magnitude of inhibition by this mechanism is comparable to Akt-mediated phosphorylation of Ser^{9} (Thornton *et al*, 2008). Interestingly, in contrast to Ser^{9} phosphorylation, Ser^{389}/Thr^{390} phosphorylation of GSK3β is detectable only in specific tissues, with the brain containing the highest level of phospho-Ser^{389} GSK3β (Thornton *et al*, 2008). Our findings here show that GSK3β Ser^{389} phosphorylation has a distinct role in restraining GSK3β activity and maintaining neuronal viability that is independent of Ser^{9} phosphorylation. While GSK3β Ser^{9} phosphorylation is detected in both the cytoplasm and the nucleus, GSK3β Ser^{389} phosphorylation is primarily nuclear. Ser^{9} phosphorylation and Ser^{389} phosphorylation are detected in different pools of GSK3β and Ser^{9} phosphorylation cannot compensate for the loss of Ser^{389} phosphorylation in the brain. The neurodegenerative phenotype found in Ser^{389}Ala GSK3β KI mice has not been reported for Ser^{9}Ala GSK3β KI mice (Hongisto *et al*, 2008; Eom and Jope, 2009). Thus, GSK3β Ser^{389} and Ser^{9} inhibitory phosphorylation regulate distinct pools of GSK3β that control different signaling pathways in the brain.

The fact that Ser^{389} and Ser^{9} phosphorylation target different physical pools of GSK3β suggests that they respond to different stimuli. Our recent studies have revealed that inactivation of GSK3β by phosphorylation on Ser^{389} is specifically triggered by DSB generated by external stimuli or endogenous processes (eg, V(D)J recombination of T-cell receptor genes in thymocytes) (Thornton *et al*, 2016). This explains why phospho-Ser^{389} GSK3β was not detected in most tissues under normal physiological conditions (Thornton *et al*, 2008). Although DNA DSB are difficult to detect in the normal brain it was believed that DSB were generated but a highly efficient DNA repair system prevented DSB from accumulating in the brain (McKinnon, 2009). A number of recent studies have provided strong evidence for the existence of DSB in the brain. Normal neuronal activity results in the generation of DSB although the mechanism of DSB induction was not examined (Suberbielle *et al*, 2013). Moreover, a subset of early-response genes in neurons requires DSB formation for their expression that is critical for the experience-driven changes associated with memory and learning (Madabhushi *et al*, 2015). It has been shown that neural stem/progenitor cells contain recurrent DSB clusters within long neural genes (Wei *et al*, 2016). Here we show that in the region where we detect enriched dark neurons in GSK3β KI mice, phospho-Ser^{389} GSK3β co-localizes with DSB marker γH2AX. It is possible that cells within the regions where dark neurons are detected in the GSK3β KI mice may define a circuit that contains cells more prone to DSB, thus more sensitive to failure to inactivate GSK3β through phosphorylation on Ser^{389}. This could explain why only specific regions and not all neurons are affected in the GSK3β KI mice. In the context of the stress-associated fear conditioning phenotype that we show here, it is interesting that exposure to stress hormones can also lead to DSB accumulation (Hara *et al*, 2011). Thus, the constitutive phosphorylation of GSK3β on Ser^{389} in the brain is likely maintained by the ongoing generation of DSB in neurons to attenuate the abundant GSK3β activity present in the brain.

Normally DSB are associated with cell death. However, we have shown that phosphorylation of GSK3β at Ser^{389} leads to increased cell survival and protecting cells from cell death caused by DSB generated by external stimuli and internal processes (Thornton *et al*, 2016). While a number of studies have addressed DSB in the brain, none have addressed how cells survive this constant generation of DSB. Here we show that inactivation of GSK3β through phosphorylation at Ser^{389} can be a novel mechanism to provide protection to prevent neuronal cell death during DSB repair. The increased cell death found in certain regions of the brain in Ser^{389}Ala GSK3β KI mice has not been reported in Ser^{9}Ala GSK3β KI mice, indicating that this is a unique mechanism to control survival in the brain. Interestingly, similar to the death induced by endogenously generated DSB in B cells, the death observed in the brains of GSK3β Ser^{389}Ala KI mice seems to be through necroptosis more than apoptosis. Necroptosis has also been reported to occur in the brain in other studies (Vitner *et al*, 2014; Zhao *et al*, 2015). Since DSB have been

reported to promote necroptosis (Biton and Ashkenazi, 2011; Tenev *et al*, 2011), failure to inactivate GSK3β through Ser^{389} phosphorylation in response to DSB likely contributes to the increased necroptosis found in the brains of GSK3β Ser^{389}Ala KI mice.

Despite the presence of hippocampal neuronal degeneration in the GSK3β Ser^{389}Ala KI mice, no impact on spatial memory or learning was observed. Locomotor activity was also normal. Failure to phosphorylate GSK3β at Ser^{389} did not affect anxiety or depression-like behavior either. However, we show that GSK3β Ser^{389}Ala KI mice display overgeneralized and persistent fear. This suggests that there may be undetermined specificity to the subset of affected neurons in GSK3β KI mice. Overgeneralization of fear and failure to extinguish responses to fear-associated cues is common in PTSD (Wessa and Flor, 2007). These altered fear responses are also found in rodent stress exposure models used to model this human disorder (Izquierdo *et al*, 2006; Baran *et al*, 2009; Hoffman *et al*, 2014). A brain circuit with the amygdala at its core and involving the hippocampus and several cortical areas (eg, frontal, entorhinal, piriform, infralimbic) is involved in fear learning and extinction. Thus, disruption of this circuit caused by dispersed neurodegeneration in GSK3β KI mice may be the underlying cause of the persistent and generalized fear phenotype. Mice with alanine substitutions blocking N-terminal Ser^{9} inhibitory phosphorylation of both GSK3β and GSK3α have been shown to have a complex behavior phenotype with an increased anxiety and depression-like phenotype (Polter *et al*, 2010). The relative contributions of the individual isoforms to this complex behavior phenotype have not been reported.

Taken together our data show that phosphorylation of GSK3β at Ser^{389} by p38 MAPK promotes the survival of a subset of neurons critical for modulating the conditioned fear response. It is important to note that there is a common polymorphism (around 48% allele frequency) in the human GSK3β gene that results in the expression of a GSKβ protein lacking the Thr^{390} regulatory site (Rs6438552). The T allele is associated with altered splicing such that exon ll (containing the coding region for Thr^{390}) is deleted (Kwok *et al*, 2005). This allele is associated with enhanced GSK3β activity and has been linked to neurodegenerative disorders such as Parkinson's disease, bi-polar disorder, and major depressive disorder (Kwok *et al*, 2005; Kalinderi *et al*, 2011; Liu *et al*, 2012; Lin *et al*, 2013; Yuan *et al*, 2013). Therefore, increased expression of GSK3β lacking the Thr^{390} inhibitory phosphorylation site in humans may impair neuronal survival and contribute to neurological disease. While interest in targeting GSK3 to treat neurological disease has been growing in recent years, the selectivity of this pathway for nuclear GSK3β (in the context of DSB) and the PTSD-like behavior observed make it a more appealing target to manipulate cell survival for specific neurodegenerative diseases. The design of new therapies that specifically target C-terminal Thr^{390} phosphorylation of nuclear GSK3β could facilitate the development strategies with potentially greater specificity.

FUNDING AND DISCLOSURE

This work was supported by NIH grant R01 AI051454 (to MR) and the Consolider grant CSD2010-00045 from the Spanish Ministerio de Economia y Competitividad (MINECO) (to ARN). The authors declare no conflict of interest.

ACKNOWLEDGMENTS

We thank the Vermont Cancer Center DNA Sequencing Facility and the University of Vermont College of Med. Microscopy Imaging Center for their services.

REFERENCES

American Psychiatric Association (2000). *Diagnostic Criteria from DSM-IV-TR*. American Psychiatric Association: Washington, DC.

Arbour N, Vanderluit JL, Le Grand JN, Jahani-Asl A, Ruzhynsky VA, Cheung EC *et al* (2008). Mcl-1 is a key regulator of apoptosis during CNS development and after DNA damage. *J Neurosci* **28**: 6068–6078.

Baran SE, Armstrong CE, Niren DC, Hanna JJ, Conrad CD (2009). Chronic stress and sex differences on the recall of fear conditioning and extinction. *Neurobiol Learn Mem* **91**: 323–332.

Beurel E, Song L, Jope RS (2011). Inhibition of glycogen synthase kinase-3 is necessary for the rapid antidepressant effect of ketamine in mice. *Mol Psychiatry* **16**: 1068–1070.

Bijur GN, De Sarno P, Jope RS (2000). Glycogen synthase kinase-3beta facilitates staurosporine- and heat shock-induced apoptosis. Protection by lithium. *J Biol Chem* **275**: 7583–7590.

Bijur GN, Jope RS (2003). Glycogen synthase kinase-3 beta is highly activated in nuclei and mitochondria. *Neuroreport* **14**: 2415–2419.

Biton S, Ashkenazi A (2011). NEMO and RIP1 control cell fate in response to extensive DNA damage via TNF-alpha feedforward signaling. *Cell* **145**: 92–103.

Bogdanova OV, Kanekar S, D'Anci KE, Renshaw PF (2013). Factors influencing behavior in the forced swim test. *Physiol Behav* **118**: 227–239.

Cai Z, Zhao Y, Zhao B (2012). Roles of glycogen synthase kinase 3 in Alzheimer's disease. *Curr Alzheimer Res* **9**: 864–879.

Carmichael J, Sugars KL, Bao YP, Rubinsztein DC (2002). Glycogen synthase kinase-3beta inhibitors prevent cellular polyglutamine toxicity caused by the Huntington's disease mutation. *J Biol Chem* **277**: 33791–33798.

Chiu CT, Scheuing L, Liu G, Liao HM, Linares GR, Lin D *et al* (2015). The mood stabilizer lithium potentiates the antidepressant-like effects and ameliorates oxidative stress induced by acute ketamine in a mouse model of stress. *Int J Neuropsychopharmacol* **18**: 1–13.

Cole AR (2013). Glycogen synthase kinase 3 substrates in mood disorders and schizophrenia. *FEBS J* **280**: 5213–5227.

Colié S, Sarroca S, Palenzuela R, Garcia I, Matheu A, Corpas R *et al* (2017). Neuronal p38α mediates synaptic and cognitive dysfunction in an Alzheimer's mouse model by controlling β-amyloid production. *Sci Rep* **7**: 45306.

Cross DA, Alessi DR, Cohen P, Andjelkovich M, Hemmings BA (1995). Inhibition of glycogen synthase kinase-3 by insulin mediated by protein kinase B. *Nature* **378**: 785–789.

Dajani R, Fraser E, Roe SM, Young N, Good V, Dale TC *et al* (2001). Crystal structure of glycogen synthase kinase 3 beta: structural basis for phosphate-primed substrate specificity and autoinhibition. *Cell* **105**: 721–732.

Davis M (2006). Neural systems involved in fear and anxiety measured with fear-potentiated startle. *Am Psychol* **61**: 741–756.

Derijard B, Hibi M, Wu IH, Barrett T, Su B, Deng T *et al* (1994). JNK1: a protein kinase stimulated by UV light and Ha-Ras that binds and phosphorylates the c-Jun activation domain. *Cell* **76**: 1025–1037.

Doble BW, Woodgett JR (2003). GSK-3: tricks of the trade for a multi-tasking kinase. *J Cell Sci* **116**: 1175–1186.

Duvarci S, Pare D (2014). Amygdala microcircuits controlling learned fear. *Neuron* **82**: 966–980.

Eldar-Finkelman H, Martinez A (2011). GSK-3 inhibitors: preclinical and clinical focus on CNS. *Front Mol Neurosci* **4**: 32.

Embi N, Rylatt DB, Cohen P (1980). Glycogen synthase kinase-3 from rabbit skeletal muscle. Separation from cyclic-AMP-dependent protein kinase and phosphorylase kinase. *Eur J Biochem* **107**: 519–527.

Eom TY, Jope RS (2009). Blocked inhibitory serine-phosphorylation of glycogen synthase kinase-3alpha/beta impairs in vivo neural precursor cell proliferation. *Biol Psychiatry* **66**: 494–502.

Filali M, Cheng N, Abbott D, Leontiev V, Engelhardt JF (2002). Wnt-3A/beta-catenin signaling induces transcription from the LEF-1 promoter. *J Biol Chem* **277**: 33398–33410.

Frame S, Cohen P (2001). GSK3 takes centre stage more than 20 years after its discovery. *Biochem J* **359**: 1–16.

Frame S, Cohen P, Biondi RM (2001). A common phosphate binding site explains the unique substrate specificity of GSK3 and its inactivation by phosphorylation. *Mol Cell* **7**: 1321–1327.

Garman RH (2011). Histology of the central nervous system. *Toxicol Pathol* **39**: 22–35.

Gilbertson MW, Shenton ME, Ciszewski A, Kasai K, Lasko NB, Orr SP *et al* (2002). Smaller hippocampal volume predicts pathologic vulnerability to psychological trauma. *Nat Neurosci* **5**: 1242–1247.

Hara MR, Kovacs JJ, Whalen EJ, Rajagopal S, Strachan RT, Grant W *et al* (2011). A stress response pathway regulates DNA damage through beta2-adrenoreceptors and beta-arrestin-1. *Nature* **477**: 349–353.

Hoeflich KP, Luo J, Rubie EA, Tsao MS, Jin O, Woodgett JR (2000). Requirement for glycogen synthase kinase-3beta in cell survival and NF-kappaB activation. *Nature* **406**: 86–90.

Hoffman AN, Lorson NG, Sanabria F, Foster Olive M, Conrad CD (2014). Chronic stress disrupts fear extinction and enhances amygdala and hippocampal Fos expression in an animal model of post-traumatic stress disorder. *Neurobiol Learn Mem* **112**: 139–147.

Hongisto V, Vainio JC, Thompson R, Courtney MJ, Coffey ET (2008). The Wnt pool of glycogen synthase kinase 3beta is critical for trophic-deprivation-induced neuronal death. *Mol Cell Biol* **28**: 1515–1527.

Izquierdo A, Wellman CL, Holmes A (2006). Brief uncontrollable stress causes dendritic retraction in infralimbic cortex and resistance to fear extinction in mice. *J Neurosci* **26**: 5733–5738.

Jacobs KM, Bhave SR, Ferraro DJ, Jaboin JJ, Hallahan DE, Thotala D (2012). GSK-3beta: a bifunctional role in cell death pathways. *Int J Cell Biol* **2012**: 930710.

Jamil S, Stoica C, Hackett TL, Duronio V (2010). MCL-1 localizes to sites of DNA damage and regulates DNA damage response. *Cell Cycle* **9**: 2843–2855.

Jope RS (2011). Glycogen synthase kinase-3 in the etiology and treatment of mood disorders. *Front Mol Neurosci* **4**: 16.

Jope RS, Johnson GV (2004). The glamour and gloom of glycogen synthase kinase-3. *Trends Biochem Sci* **29**: 95–102.

Kalinderi K, Fidani L, Katsarou Z, Clarimon J, Bostantjopoulou S, Kotsis A (2011). GSK3beta polymorphisms, MAPT H1 haplotype and Parkinson's disease in a Greek cohort. *Neurobiol Aging* **32**: 546 e541–545.

Kim JJ, Jung MW (2006). Neural circuits and mechanisms involved in Pavlovian fear conditioning: a critical review. *Neurosci Biobehav Rev* **30**: 188–202.

Kim WY, Wang X, Wu Y, Doble BW, Patel S, Woodgett JR *et al* (2009). GSK-3 is a master regulator of neural progenitor homeostasis. *Nat Neurosci* **12**: 1390–1397.

Kwok JB, Hallupp M, Loy CT, Chan DK, Woo J, Mellick GD *et al* (2005). GSK3B polymorphisms alter transcription and splicing in Parkinson's disease. *Ann Neurol* **58**: 829–839.

LeDoux J (2003). The emotional brain, fear, and the amygdala. *Cell Mol Neurobiol* **23**: 727–738.

Lin YF, Huang MC, Liu HC (2013). Glycogen synthase kinase 3beta gene polymorphisms may be associated with bipolar I disorder and the therapeutic response to lithium. *J Affect Disord* **147**: 401–406.

Liu C, Li Y, Semenov M, Han C, Baeg GH, Tan Y *et al* (2002). Control of beta-catenin phosphorylation/degradation by a dual-kinase mechanism. *Cell* **108**: 837–847.

Liu RJ, Fuchikami M, Dwyer JM, Lepack AE, Duman RS, Aghajanian GK (2013). GSK-3 inhibition potentiates the synaptogenic and antidepressant-like effects of subthreshold doses of ketamine. *Neuropsychopharmacology* **38**: 2268–2277.

Liu S, Sun N, Xu Y, Yang C, Ren Y, Liu Z *et al* (2012). Possible association of the GSK3beta gene with the anxiety symptoms of major depressive disorder and P300 waveform. *Genet Test Mol Biomarkers* **16**: 1382–1389.

Long PM, Stradecki HM, Minturn JE, Wesley UV, Jaworski DM (2011). Differential aminoacylase expression in neuroblastoma. *Int J Cancer* **129**: 1322–1330.

Lovestone S, Boada M, Dubois B, Hull M, Rinne JO, Huppertz HJ *et al* (2015). A phase II trial of tideglusib in Alzheimer's disease. *J Alzheimer's Dis* **45**: 75–88.

Madabhushi R, Gao F, Pfenning AR, Pan L, Yamakawa S, Seo J *et al* (2015). Activity-induced DNA breaks govern the expression of neuronal early-response genes. *Cell* **161**: 1592–1605.

Maren S (2001). Neurobiology of Pavlovian fear conditioning. *Annu Rev Neurosci* **24**: 897–931.

Maurer U, Charvet C, Wagman AS, Dejardin E, Green DR (2006). Glycogen synthase kinase-3 regulates mitochondrial outer membrane permeabilization and apoptosis by destabilization of MCL-1. *Mol Cell* **21**: 749–760.

McKinnon PJ (2009). DNA repair deficiency and neurological disease. *Nat Rev Neurosci* **10**: 100–112.

McManus EJ, Sakamoto K, Armit LJ, Ronaldson L, Shpiro N, Marquez R *et al* (2005). Role that phosphorylation of GSK3 plays in insulin and Wnt signalling defined by knockin analysis. *EMBO J* **24**: 1571–1583.

Morris RG, Garrud P, Rawlins JN, O'Keefe J (1982). Place navigation impaired in rats with hippocampal lesions. *Nature* **297**: 681–683.

Niehrs C, Acebron SP (2010). Wnt signaling: multivesicular bodies hold GSK3 captive. *Cell* **143**: 1044–1046.

Noble W, Planel E, Zehr C, Olm V, Meyerson J, Suleman F *et al* (2005). Inhibition of glycogen synthase kinase-3 by lithium correlates with reduced tauopathy and degeneration in vivo. *Proc Natl Acad Sci USA* **102**: 6990–6995.

Palomo V, Martinez A (2016). Glycogen synthase kinase 3 (GSK-3) inhibitors: a patent update (2014-2015). *Expert Opin Ther Pat* **27**: 657–666.

Polter A, Beurel E, Yang S, Garner R, Song L, Miller CA *et al* (2010). Deficiency in the inhibitory serine-phosphorylation of glycogen synthase kinase-3 increases sensitivity to mood disturbances. *Neuropsychopharmacology* **35**: 1761–1774.

Rincon M, Derijard B, Chow CW, Davis RJ, Flavell RA (1997). Reprogramming the signalling requirement for AP-1 (activator protein-1) activation during differentiation of precursor CD4+ T-cells into effector Th1 and Th2 cells. *Genes Funct* **1**: 51–68.

Rockenstein E, Torrance M, Adame A, Mante M, Bar-on P, Rose JB *et al* (2007). Neuroprotective effects of regulators of the glycogen synthase kinase-3beta signaling pathway in a transgenic model of Alzheimer's disease are associated with reduced amyloid precursor protein phosphorylation. *J Neurosci* **27**: 1981–1991.

Rodriguez DA, Weinlich R, Brown S, Guy C, Fitzgerald P, Dillon CP *et al* (2015). Characterization of RIPK3-mediated phosphorylation of the activation loop of MLKL during necroptosis. *Cell Death Differ* **23**: 76–88.

Schmued LC, Stowers CC, Scallet AC, Xu L (2005). Fluoro-Jade C results in ultra high resolution and contrast labeling of degenerating neurons. *Brain Res* **1035**: 24–31.

Schreiber E, Matthias P, Muller MM, Schaffner W (1989). Rapid detection of octamer binding proteins with 'mini-extracts', prepared from a small number of cells. *Nucleic Acids Res* **17**: 6419.

Sheline YI, Sanghavi M, Mintun MA, Gado MH (1999). Depression duration but not age predicts hippocampal volume loss in medically healthy women with recurrent major depression. *J Neurosci* **19**: 5034–5043.

Stambolic V, Woodgett JR (1994). Mitogen inactivation of glycogen synthase kinase-3 beta in intact cells via serine 9 phosphorylation. *Biochem J* **303**(Pt 3): 701–704.

Suberbielle E, Sanchez PE, Kravitz AV, Wang X, Ho K, Eilertson K *et al* (2013). Physiologic brain activity causes DNA double-strand breaks in neurons, with exacerbation by amyloid-beta. *Nat Neurosci* **16**: 613–621.

Tait SW, Ichim G, Green DR (2014). Die another way—non-apoptotic mechanisms of cell death. *J Cell Sci* **127**: 2135–2144.

Tenev T, Bianchi K, Darding M, Broemer M, Langlais C, Wallberg F *et al* (2011). The Ripoptosome, a signaling platform that assembles in response to genotoxic stress and loss of IAPs. *Mol Cell* **43**: 432–448.

Thornton TM, Delgado P, Chen L, Salas B, Krementsov D, Fernandez M *et al* (2016). Inactivation of nuclear GSK3[beta] by Ser389 phosphorylation promotes lymphocyte fitness during DNA double-strand break response. *Nature Commun* **7**: 1–12.

Thornton TM, Pedraza-Alva G, Deng B, Wood CD, Aronshtam A, Clements JL *et al* (2008). Phosphorylation by p38 MAPK as an alternative pathway for GSK3beta inactivation. *Science* **320**: 667–670.

Tugores A, Alonso MA, Sanchez-Madrid F, de Landazuri MO (1992). Human T cell activation through the activation-inducer molecule/CD69 enhances the activity of transcription factor AP-1. *J Immunol* **148**: 2300–2306.

Vitner EB, Salomon R, Farfel-Becker T, Meshcheriakova A, Ali M, Klein AD *et al* (2014). RIPK3 as a potential therapeutic target for Gaucher's disease. *Nat Med* **20**: 204–208.

Wei PC, Chang AN, Kao J, Du Z, Meyers RM, Alt FW *et al* (2016). Long neural genes harbor recurrent DNA break clusters in neural stem/progenitor cells. *Cell* **164**: 644–655.

Wessa M, Flor H (2007). Failure of extinction of fear responses in posttraumatic stress disorder: evidence from second-order conditioning. *Am J Psychiatry* **164**: 1684–1692.

Woodgett JR (1990). Molecular cloning and expression of glycogen synthase kinase-3/factor A. *EMBO J* **9**: 2431–2438.

Yuan Y, Tong Q, Zhou X, Zhang R, Qi Z, Zhang K (2013). The association between glycogen synthase kinase 3 beta polymorphisms and Parkinson's disease susceptibility: a meta-analysis. *Gene* **524**: 133–138.

Zhao H, Jaffer T, Eguchi S, Wang Z, Linkermann A, Ma D (2015). Role of necroptosis in the pathogenesis of solid organ injury. *Cell Death Dis* **6**: e1975.

Supplementary Information accompanies the paper on the Neuropsychopharmacology website (http://www.nature.com/npp)